# Dynamic cycling and redox transformations of dissolved organic sulfur in the surface ocean

Molly A. Crotteau[1], Erin L. McParland[2,3], Alexandra A. Phillips[1,4], Elizabeth B. Kujawinski[3], Krista Longnecker[3], Aaron M. Martinez[5], Samuel M. Webb[6], Morgan R. Raven[1,5]

## Affiliations

[1]Earth Science Department, University of California Santa Barbara, Santa Barbara, CA, United States of America.

[2]College of Earth, Ocean, and Atmospheric Sciences, Oregon State University, Corvallis, OR, United States of America.

[3]Department of Marine Chemistry and Geochemistry, Woods Hole Oceanographic Institution, Woods Hole, MA, United States of America.

[4]Bren School of Environmental Science and Management, University of California Santa Barbara, Santa Barbara, CA, United States of America.

[5]Marine Science Institute, University of California Santa Barbara, Santa Barbara, CA, United States of America.

[6]Stanford Synchrotron Radiation Lightsource, Stanford University, Menlo Park, California, United States of America.

## Contact Information

Molly A. Crotteau (corresponding author): mollycrotteau@ucsb.edu, ORCID: 0000-0001-7888-0093

Erin L. McParland: erin.mcparland@oregonstate.edu, ORCID: 0000-0003-1734-8938

Alexandra A. Phillips: alexandra_phillips@ucsb.edu, ORCID: 0000-0001-5959-5238

Elizabeth B. Kujawinksi: ekujawinski@whoi.edu, ORCID: 0000-0001-8261-971X

Krista Longnecker: klongnecker@whoi.edu, ORCID: 0000-0002-6850-2694

Aaron M. Martinez: aaronmartinez@ucsb.edu, ORCID: 0000-0001-5761-8926

Samuel M. Webb: samwebb@slac.stanford.edu, ORCID: 0000-0003-1188-0464

Morgan R. Raven: raven@ucsb.edu, ORCID: 0000-0003-4953-9966

**Running Head**

*Dissolved organic sulfur cycling*

**Keywords**

Dissolved organic sulfur, dissolved organic matter, sulfur isotopes, x-ray absorption spectroscopy, microbial loop

## Abstract

The marine dissolved organic sulfur (DOS) pool contains both labile metabolites that are rapidly cycled in the surface ocean and compounds that may persist for thousands of years in the marine environment. Here, we describe the sulfur speciation of solid-phase extracted marine DOS ($DOS_{SPE}$) from the North Atlantic surface ocean, revealing a diversity of oxidation states that include alkyl sulfides, disulfides, aromatics, sulfonates, and sulfate esters. As dissolved organic carbon concentrations decrease with depth in the water column, relative abundances of reduced sulfur species decrease while those of oxidized sulfur species increase, indicating preferential remineralization of reduced organic sulfur compounds. Although microorganisms are considered to be the origin of a vast majority of marine $DOS_{SPE}$, the $DOS_{SPE}$ produced by cultures of phototrophs and heterotrophic bacteria is compositionally distinct and $^{34}S$-enriched relative to environmental $DOS_{SPE}$. Ultimately, mechanisms spanning different timescales, including microbial reworking, uptake, and photochemical oxidation transform labile DOS in the surface ocean, and may generate recalcitrant compounds that contribute to the long-lived dissolved organic matter pool. The oxidation states of organic sulfur function as powerful tools for tracking the sources, sinks, and transformations of organic matter in complex biogeochemical systems.


## Introduction

A significant proportion of dissolved organic matter (DOM) in the ocean resists breakdown for thousands of years and may impact climate on glacial – interglacial timescales by acting as a long-term reservoir for carbon (Hansell 2013). Despite ongoing progress toward characterizing DOM with new techniques (i.e., Kujawinski et al. 2004; Hertkorn et al. 2013; Petras et al. 2017), we do not yet understand the sources of this recalcitrant material in the ocean. Sulfur (S) is a

primary constituent of photosynthetic biomass (C:S ~ 95:1) (Ho et al. 2003), and organic sulfur (OS) likewise contributes to the marine DOM pool (Koch et al. 2017; Phillips et al. 2022). However, dissolved organic sulfur (DOS) is a molecularly complex pool that spans a broad spectrum of reactivity (Valle et al. 2015; Clifford et al. 2017; Buck-Wiese et al. 2023), and its relationship to DOM recalcitrance is unknown.

Labile, rapidly cycled OS compounds play essential roles in marine ecosystems as nutrient and energy sources. Heterotrophic bacteria and other microorganisms can oxidize DOS for metabolic energy (Moran and Durham 2019), while others assimilate OS for biosynthesis (Tripp et al. 2008). Many ubiquitous metabolites with reduced and oxidized S functional groups are rapidly cycled and consumed by microbes in the marine environment; their concentrations are generally low and decrease with depth over the top 125 m of the surface ocean (Kiene and Linn 2000; Valle et al. 2015; Sabadel et al. 2017). For example, concentrations of methionine, an alkyl sulfide, range from < 50 pM to ~2 nM (Valle et al. 2015; Sabadel et al. 2017); concentrations of other thiol-containing metabolites, such as cysteine and glutathione, range from 1 – 15 nM (Dupont et al. 2006). Similar concentrations have been observed for oxidized S-bearing metabolites: concentrations of taurine, an amino acid critical for osmoregulation, reach 10 nM in surface waters (Clifford et al. 2017), and concentrations of sulfoquinovosyl diacylglycerol (SQDG), an important membrane lipid, reach at least ~12 nM (Brandsma et al. 2012). OS-containing osmolytes, such as 2,3-dihydroxypropane-1-sulfonate (DHPS) and dimethylsulfoniopropionate (DMSP), are two abundant OS molecules found at mM concentrations in primary producers. DMSP, which accounts for ~5 – 9% of carbon produced by marine phytoplankton (Galí et al. 2015), can be broken down by heterotrophic bacteria and converted to dimethyl sulfide (DMS), which can be lost from the surface ocean via volatilization (Lana et al. 2011; Zhang et al. 2019; Wohl et al. 2024). Large

amounts of DMS (28 Tg S/yr) are emitted to the atmosphere annually, where it impacts cloud formation and local climate (Lana et al. 2011; Wohl et al. 2024). The link between this rapidly cycled, labile DOS and more long-lived recalcitrant DOM remains poorly understood.

Although the mechanisms may be complex, some biogenic OS compounds do appear to contribute to long-lived DOM. For example, algae contribute significantly to the DOS pool through the exudation of sulfur-rich compounds, such as fucoidan, which persists in the ocean and may be a pathway for long-term carbon preservation (Buck-Wiese et al. 2023). The transformation of OS via the microbial carbon pump and zooplankton grazing may influence overall DOM recalcitrance and may contribute to the production of long-lived DOM (Hansell 2013; Johnston et al. 2022; Moran et al. 2022). Photochemical processes also play a key role in DOS production, transformation, and loss (Riedel et al. 2016; Kieber et al. 2024). The photochemical products of DOM degradation include both volatile DOS compounds (e.g., carbonyl sulfide (OCS), carbon disulfide ($CS_2$)) and non-volatile DOS compounds (methanesulfonic acid (MSA), methanesulfinic acid (MSIA)), and sulfate (Cutter et al. 2004; Lennartz et al. 2019; Ossola et al. 2019).

Additionally, DOS can be produced and altered through geopolymerization, a broad category of polymerization and recombination reactions that enhance OM stability. Sulfurization is a special type of these reactions that occurs in anoxic environments like many coastal sediments (Pohlabeln et al. 2017; Abdulla et al. 2020). High concentrations of DOS are observed in coastal sediment porewaters, leading to the hypothesis that significant quantities of sulfurized DOM efflux from anoxic sediments (13 – 200 Tg DOS/year) (Pohlabeln et al. 2017; Raven 2025). DOM rapidly undergoes sulfurization reactions at room temperature in sulfidic conditions (Pohlabeln et al. 2017). Given these large fluxes, sulfurized DOM from sediment porewater could account for a large portion of the marine DOM pool (Pohlabeln and Dittmar 2015). However, the S isotopic

composition of DOM indicates that biogenic DOS sources, rather than sulfurized porewater DOM, comprise >90% of the water column pool of DOS (Phillips et al. 2022; Ibrahim and Tremblay 2023; Tang and Liu 2023). Like biogenic DOS, sulfurized DOM may be lost due to oxidation to sulfate through heterotrophic metabolisms or photochemical reactions (Riedel et al. 2016; Kieber et al. 2024).

Sulfur-containing biomolecules exist in a diverse range of nominal oxidation states, ranging from thiols (-2) to sulfate esters (+6) (Moran and Durham 2019). Here, we categorize reduced groups to include alkyl sulfides (R–S–R), disulfides (R–S–S–R), and aromatic S. The alkyl sulfide pool also includes thiols (R–SH) and sulfonium compounds ($[SR_3]^+$) that are indistinguishable via XAS. Oxidized groups include sulfoxides (R–SO–R), sulfonates and sulfones, ($R–SO_3^-$ and $R–SO_2–R$), and sulfate esters ($R–O–SO_3^-$). Many of the important transformations in the DOS pool likely involve changes in the oxidation state of sulfur. Accordingly, we use x-ray absorption spectroscopy (XAS), which provides information on S oxidation state, in conjunction with elemental ratios and S isotopes, to reveal the diversity of OS molecules within the marine DOM pool. To better understand the biogenic sources of marine solid-phase extracted DOS ($DOS_{SPE}$) and the processes that transform it in the environment, such as oxidation, photochemistry, and microbial re-working, we describe the S speciation and isotopic composition of open ocean marine $DOS_{SPE}$ for a suite of depth profiles in the North Atlantic. We then compare these marine samples to extractable OS produced in-culture by select marine primary producers and heterotrophs. We also present the results of incubations that track heterotrophic microbes' transformation of primary biogenic $DOS_{SPE}$ using ultrahigh-resolution mass spectrometry. Ultimately, our results underscore the chemical diversity of DOS species and reveal first-order patterns in their spatial distributions in the surface ocean.

## Materials and Methods

### Marine sample collection

Water samples for $DOM_{SPE}$ extraction were collected on cruise AR62 on R/V *Neil Armstrong* in November 2021 from the North Atlantic along the Northeast continental shelf. Three-point depth profiles were collected from seven stations; three stations were on the shelf and four stations were off the shelf (Fig. 1). The shallowest sample at all stations was a surface sample at 5 m depth. The mid-point depth sample was collected from below the relative chlorophyll maximum where oxygen decreased at all stations, as determined by CTD casts (Fig S1). The deep samples were collected from 70 – 150 m water depth on the shelf and 200 m off the shelf. Maximum water depth off the shelf was 2685 m. For depth comparisons, surface samples are defined as <10 m depth, mid-depth samples are samples collected from 30 – 80 m, and deep samples were collected below 150 m.

Seawater (~10 L) was collected from Niskin bottles with silicone tubing into acid-rinsed polycarbonate carboys and passed through a 0.7 μm combusted GF/F filter using a peristaltic pump with Teflon tubing. A subsample of 20 mL of filtrate was collected into combusted glass EPA vials with Teflon lids, acidified to pH 2 with concentrated OmniTrace hydrochloric acid (12 N), and stored at 4 °C (Halewood et al. 2022). Non-purgeable dissolved organic carbon (DOC), which contains no volatile compounds (DMS is not present in these samples), was measured with high-temperature combustion (Halewood et al. 2022). The remaining filtrate was retained for $DOM_{SPE}$ isolation.

143 **Monocultures**

144 Artificial seawater amended with macronutrients, trace metals, and vitamins with
145 respective media recipes was used to grow monocultures of *Prochlorococcus marinus* CCMP2971
146 (Pro99 media), *Thalassiosira pseudonana* CCMP1335 (f/2+Si media), *Ruegeria pomeroyi* DSS-3
147 (ProMM media), and *Alteromonas macleodii* MIT1002 (ProMM media) (Guillard and Ryther
148 1962; Guillard 1975; Moore et al. 2007). After achieving steady-state growth conditions defined
149 by three consistent growth rates calculated across successive transfers, monocultures were sampled
150 in the late exponential phase. Cultures were centrifuged (3000 x *g* for 15 min at room temperature)
151 to isolate cells from exudates. To rinse away excess sulfate, pellets were centrifuged and
152 resuspended in sulfate-free artificial seawater three times. The rinsed pellets were frozen at -20 ℃.
153 The exudates were filtered with a peristaltic pump through an acid-rinsed 0.2 μm PTFE filter
154 (Omnipore, EMD Millipore). Exudate $DOM_{SPE}$ isolation is described below.

155 **OS transformation incubations**

156 Cells were harvested from the two phototroph monocultures (*Prochlorococcus marinus*
157 and *Thalassiosira pseudonana*) via centrifugation and subsequently lysed by sonication on ice and
158 subjected to three freeze-thaw cycles. The lysates were centrifuged (20,000 x *g* for 15 min at 4℃)
159 and the concentrated DOM of the supernatant was used as the sole carbon source for incubation of
160 heterotrophic bacteria. The two heterotrophic bacteria (*Ruegeria pomeroyi* and *Alteromonas*
161 *macleodii*) were grown as monocultures in artificial seawater amended with macronutrients, trace
162 metals, vitamins, and the respective lysate. Cultures were grown in these conditions over multiple
163 dilutions and then the experiment was inoculated as three biological replicates. Growth was

monitored by counting SYBR Green-stained cells with flow cytometry. $DOM_{SPE}$ was sampled at the initiation of the experiment and as cells approached stationary phase.

**$DOM_{SPE}$ isolation**

For filtrates from monoculture experiments and *in situ* sampling, filtrate was acidified to a pH of 2 with concentrated (12 N) OmniTrace hydrochloric acid and concentrated via solid phase extraction (SPE) with styrene-divinylbenzene polymer resin columns (Bond Elut PPL, Agilent, Santa Clara) following established protocols (Dittmar et al. 2008; Phillips et al. 2022). Briefly, the SPE column was primed with methanol, the filtrate was passed onto the column via FEP tubing (Thermo Scientific) and an extraction manifold, the column was rinsed five times with 0.01M HCl to remove sulfate; sulfate removal was confirmed via XAS. The samples were eluted into combusted amber glass vials with 6 mL methanol. Samples were evaporated under $N_2$ to near dryness and stored at -20°C. Media blanks were also passed through SPE columns for all monoculture experiments.

The DOS molecules studied here represent only those that are retained on SPE resin. For DOC, recovery from SPE on PPL is variable (37 – 74%), while DON recovery is lower (10 – 40%) (Broek et al., 2017; Dittmar et al., 2008; Hertkorn et al., 2013). DOS recovery is uncertain, with extraction efficiencies ranging from 0 – >90% for a subset of S-containing marine metabolites, but SPE resins are particularly effective for extracting relatively large, uncharged, slightly polar (100 – 1000 Da) OS compounds (Johnson et al. 2017). Improved constraints on the impact of PPL on both S speciation and isotopic composition would be valuable in applying these data to the broader DOS and DOM pools.

**EA-IRMS**

186 $DOS_{SPE}$ samples were transferred in methanol to smooth-walled ultra-clean tin EA capsules
187 (6 x 2.9 mm, OEA Laboratories) (Phillips et al. 2022). Methanol was evaporated at room
188 temperature (~3 h) and sample tins were folded closed. C and S contents and $\delta^{13}C$ values of
189 $DOM_{SPE}$ were determined with an elemental analyzer coupled to an isotope ratio mass
190 spectrometer (EA-IRMS; Elementar Vario Isotope Select EA interfaced to a Nu Horizon IRMS)
191 with He carrier gas (200 mL/min). $CO_2$ and $SO_2$ were quantified using a thermal conductivity
192 detector (TCD). C and S abundances were calibrated using a sulfanilamide standard curve (1.5 –
193 35 μmole C; 0.25 – 6 μmole S) run in duplicate ($R^2$ for C and S calibration curves > 0.99). Sample
194 $\delta^{13}C$ values were calibrated using carbon isotope standards USGS-61 (-35.05‰), 62 (-14.79‰),
195 and 63 (-1.17‰) run in triplicate and are reported relative to Vienna Pee Dee Belemnite (VPDB).

196 S isotope analyses were conducted on EA IsoLink combustion EA coupled to a Delta V
197 Plus IRMS via a ConFlo IV Universal interface (all from Thermo Scientific) (Phillips et al. 2021,
198 2022). $CO_2$ was diluted at the highest setting (88%) due to high C contents using the ConFlo; $SO_2$
199 was not diluted. $DOS_{SPE}$ samples containing 5 μg S determined from measured S content were
200 prepared in tin EA capsules as described above. S isotopes were calibrated using IAEA silver
201 sulfide standards S-1 (-0.30‰), S-2 (22.62‰), and S-3 (-32.49‰) and are reported with respect
202 to the Vienna Canyon Diablo Troilite (VCDT). Media blanks passed through SPE columns were
203 also analyzed via EA-IRMS; these blanks did not contain detectable S.

204 Given sample size limitation, we were only able to make single or duplicate measurements
205 for each sample. Monoculture $DOM_{SPE}$ samples contained very low amounts of S, so $DOM_{SPE}$
206 from the triplicate monoculture experiments were pooled to have sufficient S (2 μg) for an isotope
207 measurement. To estimate uncertainty for $\delta^{13}C_{VPDB}$, $\delta^{34}S_{VCDT}$, and C:S analyses, $DOM_{SPE}$
208 previously collected off the Scripps Pier in bulk (~200 L) was used as a consistency standard

(Phillips et al. 2022). Five Scripps $DOM_{SPE}$ samples were analyzed daily, and the standard error of each sample was calculated by dividing the standard deviation of Scripps $DOM_{SPE}$ standard measurements by the square root of the number of replicates analyzed. Standard errors of $\delta^{13}C_{VPDB}$, $\delta^{34}S_{VCDT}$, and C:S analyses were <0.1‰, <0.3‰, and ≤3%, respectively. Details on number of replicates and standard error are provided for each marine sample in Supplemental Dataset S1 and for each monoculture experiment in Supplemental Dataset S2.

**XAS analysis**

Sulfur K-edge x-ray absorption spectroscopy/x-ray fluorescence (XAS/XRF) was used to describe the bonding environment and redox state of S within bulk $DOS_{SPE}$ samples (Vairavamurthy 1998). DOS samples were suspended in 100 µL 20:1 dichloromethane : methanol and sonicated until dissolved (~10 min). Aliquots of 5% of the sample were dried at room temperature onto combusted quartz microscope slides (Chemglass). Spectra were collected at the Stanford Synchrotron Radiation Lightsource (SSRL) on beamline 14-3, which utilizes a Si(111) (Φ = 90) double crystal monochromator to achieve beam energies ranging from 2460 to 2540 eV, calibrated to the thiol pre-edge peak of thiosulfate at 2472.02 eV. Replicate spectra for each sample were acquired using a ~500 x 500 µm beam to optimize S counts and processed with the SMAK and SIXPACK software packages (Webb 2005) using a set of in-house OS standards (Fig. S1). Fit uncertainties are ± <2% (Vairavamurthy 1998).

**Mass spectrometry**

$DOM_{SPE}$ from heterotrophic bacteria incubations was analyzed as described previously (Kido Soule et al. 2015; Weber et al. 2020). Chromatography was performed using an ultrahigh-performance liquid chromatography system (Vanquish UHPLC, Thermo Scientific) coupled with an Orbitrap Fusion Lumos Tribrid mass spectrometer (Thermo Fisher Scientific). Ultra-high

performance liquid chromatography electrospray ionization tandem mass spectrometry (UHPLC-ESI-MSMS) was used to assign putative S oxidation states to $DOS_{SPE}$ features and to compare changes in their abundances from early to late exponential phase during monoculture incubation experiments. Samples were run in both positive and negative ionization mode. Details of instrument parameters and post-processing are described in the Supplement. Elemental formulas were assigned to the resulting feature table with Formularity, MFAssignR, and Sirius. If a formula was assigned by more than one algorithm, the formulas were required to match. Potential duplicate features formed as [M+H] or [M-H] adducts in both ionization modes were dereplicated by calculating and comparing the neutral masses (± 5ppm error) and retention times (± 3 seconds). Features were filtered by requiring a log2 fold-difference between the average feature intensities in samples and the MQ blank to be > 3, a < 25% relative standard deviation in the pool samples (n = 7 injections), and a S assigned to the elemental formula. Putative oxidation states were assigned (< 3 ppm) based on presence of the fragment (± electron) exact mass or a neural loss exact mass (Table S6).

## Results

### Marine samples

Samples from the top 200 m of the water column were collected from stations both on and off the continental shelf in the North Atlantic Ocean (Fig. 1A-B). CTD profiles of oceanographic parameters were collected at each station (Fig. S1). DOC concentrations decreased with depth, from 61.3 – 76.2 μM in surface water (<10 m) to 51.6 – 55.3 μM at depth (152–205 m) (Fig. 1C). Across all depths, on-shelf samples had higher DOC concentrations (71 ± 8 μM) (average ± standard deviation) than off-shelf samples (61 ± 7 μM) (one-tailed t-test p value = 0.004) (Table

S1). $DOM_{SPE}$ C:S molar ratios increased from 243 ± 22 at the surface to 289 ± 18 at depth (>150 m) ($p = 0.002$; one-tailed t-test). On-shelf samples contained more sulfur relative to carbon (C:S = 226 ± 21) than off-shelf samples (C:S = 263 ± 32) ($p = 0.003$; one-tailed t-test) (Fig. 1D; Table S2). DOS concentrations were calculated by dividing DOC concentrations by the molar C:S ratio of the corresponding $DOM_{SPE}$ sample (Ksionzek et al. 2016; Phillips et al. 2022). This calculation assumes that the extraction efficiencies for DOS and DOC are similar, i.e., that the SPE retention of larger molecules can be largely controlled by molecular properties other than lower-abundance, S-bearing functional groups. Like DOC, calculated concentrations of DOS decreased with depth, from 214 – 350 nM in surface water (<10 m) to 172 – 195 nM at depth (152–205 m) (Fig. 1E; Table S3).

$DOM_{SPE}$ $\delta^{13}C$ values became slightly more $^{13}C$ enriched with depth (Fig. 1F), increasing from -23.9 ± 0.3‰ in surface (<10 m) samples to -23.2 ± 0.2‰ at >150 m depth. On-shelf samples had slightly more negative $DOM_{SPE}$ $\delta^{13}C$ values (-24.1 ± 0.4‰) than off-shelf samples (-23.4 ± 0.3‰) ($p = 0.0007$; one-tailed t-test). $DOM_{SPE}$ $\delta^{34}S$ values were more variable, with a range of >5‰, and showed no trend with depth (Fig. 1G). $DOM_{SPE}$ $\delta^{34}S$ values averaged 15.6 ± 1.1‰ in surface (<10 m) samples and 15.7 ± 1.5‰ in deeper (>30 m) samples. However, on-shelf samples were $^{34}S$ depleted relative to off-shelf samples ($p < 0.001$; one-tailed t-test), with on-shelf samples averaging 14.9 ± 1.3‰ and off-shelf samples averaging 16.3 ± 1.1‰ (Table S2).

All marine $DOS_{SPE}$ samples contained disulfides, alkyl sulfides, aromatics, sulfonates, and sulfate esters (Fig. 2). In all samples, sulfonates and aromatics comprised a majority of the total (Fig. 3). However, the relative proportions of all oxidation states changed as a function of depth. In surface waters (< 10 m depth), $DOS_{SPE}$ was composed of an average of 10% disulfides, 10% alkyl sulfides, 28% aromatics, 2% sulfoxides, 38% sulfonates, and 12% sulfate esters (Fig. 3, Table

S4). In contrast, deeper (>150 m) $DOS_{SPE}$ contained a higher proportion of sulfonates and a smaller proportion of alkyl sulfides and disulfides, with an average composition of 4% disulfides, 4% alkyl sulfides, 24% aromatics, 2% sulfoxides, 47% sulfonates, and 19% sulfate esters (Fig. 3, Table S4). The relative abundances of OS oxidation states for individual samples correlated with DOC concentrations (Fig. 2). The relative abundances of oxidized OS species (sulfoxides, sulfonates, and sulfate esters) were negatively correlated with DOC concentration, while reduced species (aromatics, disulfide, and alkyl sulfides) showed a positive correlation. Correlations with DOC concentration were strongest for disulfides ($R^2 = 0.92$, $p < 0.00001$) and alkyl sulfides ($R^2 = 0.83$, $p < 0.00001$).

We used calculated DOS concentrations and the relative abundance of each OS species determined from XAS to estimate the concentration of each OS species in the environment (Fig. 3). As total DOS concentrations decreased with depth, oxidized OS groups that increased in relative proportion showed small decreases in concentration, while reduced OS groups that decreased in relative proportion showed larger concentration decreases. Concentrations of disulfides and alkyl sulfides ranged from 6–48 nM S and 5–51 nM S, respectively; these groups also exhibited the largest decrease in concentration with depth, from 31 ± 11 nM S and 31 ± 15 nM S in surface waters to 7 ± 1 nM S and 8 ± 1 nM S below 150 m, respectively. The concentration of aromatic S ranged from 41–113 nM S, and declined with depth, from 84 ± 18 nM OS at the surface to 44 ± 2 nM OS below 150 m. The sulfoxide concentration range of 4 ± 2 nM S was the lowest of all S species and did not change with depth. Sulfonates ranged from 83–131 nM S, with concentrations decreasing slightly with depth, from an average of 110 ± 14 nM OS in surface samples (>5 m) to an average of 88 ± 5 nM OS below 150 m. Sulfate ester concentrations ranged from 22–55 nM S and showed less variation in concentration with depth than other species. All

OS species concentrations exhibited a statistically significant difference between pooled samples from the surface (<10 m) and mid depth (30 – 80 m), and from the mid-depth and deep (>150 m) (one-way ANOVA, Tukey HSD test), except for sulfoxides and sulfate esters (Table S5). Sulfoxides exhibited no significant difference among the depth groups, whereas sulfate ester concentrations were uniquely higher in the mid-depth group than the surface group ($p = 0.03$; Table S5).

There were also notable differences between on-and off-shelf stations in reduced S species calculated concentrations (Fig. S2). The average total concentrations of disulfides and alkyl sulfides across all depths were significantly higher at shelf stations than off-shelf stations (t-test, $p < 0.001$). Disulfide and alkyl sulfide concentrations on the shelf were 37.5 ± 10.9 nM S and 37.7 ± 12.8 nM S, respectively. Off the shelf, average concentrations of disulfides (15.1 ± 7.7 nM S) and alkyl sulfides (13.8 ± 6.1 nM S) were approximately half of on-shelf values. Aromatic S was also more abundant on the shelf (94.5 ± 20.6 nM S) than off the shelf (60.3 ± 14.8 nM S) (t-test, $p < 0.001$). In contrast, the concentrations of oxidized S species remained consistently high, with no significant difference (t-test, $p = 0.99$) between on- and off-shelf stations. Similarly, sulfoxide concentrations remained consistently low (0–6 nM S) at both on- and off-shelf stations (t-test, $p > 0.01$). Sulfonate concentrations were not significantly different between on-shelf (106.5 ± 11.9 nM S) and off-shelf stations (103.8 ± 14.2 nM S). Sulfate ester concentrations were lower than sulfonate concentrations, but also were consistent between on- (37.7 ± 8.1 nM S) and off-shelf stations (39.0 ± 9.7 nM S).

**Monoculture samples**

XAS-derived OS speciation, averaged from three biological replicates, was measured in $DOM_{SPE}$ collected from monocultures grown in artificial seawater in late exponential phase, so all detected OS can be assumed to be biotically released (Fig. 4A). Within the $DOM_{SPE}$ of the heterotrophic bacteria *Ruegeria pomeroyi* and *Alteromonas macleodii*, the relative proportions of OS species and their oxidation states was consistent, averaging 15 ± 3% disulfides, 32 ± 4% alkyl sulfides, 9 ± 6% aromatics, 23 ± 9% sulfoxides, 5 ± 5% sulfonates, and 16 ± 11% sulfate esters. The $DOM_{SPE}$ released from the diatom *Thalassiosira pseudonana* was similar to the composition of heterotrophic bacteria except that it contained a notable abundance of sulfonates (~31%) compared to the other monoculture samples. $DOM_{SPE}$ from the cyanobacteria *Prochlorococcus* contained a lower proportion of OS with oxidized oxidation states (sulfoxides and sulfonates) and a higher proportion of OS with reduced oxidation states (29% disulfides and 45% alkyl sulfides) than $DOM_{SPE}$ of the heterotrophic bacteria and diatom monocultures.

$DOM_{SPE}$ samples, which were pooled from triplicate cultures to yield sufficient S for isotopic analysis, were compared with particulate biomass from each culture. The $\delta^{34}S$ values for monoculture $DOM_{SPE}$ and bulk biomass samples are reported relative to the $\delta^{34}S$ value of the growth media sulfate, which is the source of sulfur for biosynthesis (Fig. 4A). $DOM_{SPE}$ released by all monocultures was consistently $^{34}S$ enriched relative to sulfate, and $DOM_{SPE}$ exuded from the phototrophs was more $^{34}S$-enriched (6.4 – 8.6‰) than the $DOM_{SPE}$ exuded from the heterotrophic bacteria (0.1 – 2.3‰). In contrast, the particulate biomass was consistently $^{34}S$ depleted (by 5.7 to 2.1‰) relative to sulfate. Biomass was $^{34}S$-depleted relative to $DOM_{SPE}$ in all monocultures. Accounting for the abundance of OS in $DOM_{SPE}$ and the solid biomass pool, the S-isotope ratios for total biogenic production remains $^{34}S$-depleted relative to the sulfate source (Supplemental Text S3).

Finally, to understand the potential transformation of freshly produced OS by marine heterotrophic bacteria, we tracked molecular-level changes of $DOM_{SPE}$ over the course of incubations with heterotrophic bacteria (via UHPLC-ESI-MSMS). Using the same model organisms described above, lysate from each phototroph monoculture was provided as the sole carbon source to heterotroph monocultures resulting in four experimental conditions (*Alteromonas* grown on *Prochlorococcus* lysate, *Alteromonas* grown on *Thalassiosira* lysate, *Ruegeria* grown on *Prochlorococcus* lysate, and *Ruegeria* grown on *Thalassiosira* lysate) (Fig. S3). We identified 42 putative OS-containing features showing relative change between the early and late exponential phase (Fig. 4B), largely in positive ionization mode. We detected more putatively reduced DOS features (n = 30) than oxidized DOS features (n = 12). From early exponential to late exponential phase, a majority of the identified DOS features declined significantly in abundance (log2 fold-change > 2, t-test p-value ≤ 0.05), including both reduced and oxidized examples. We also observed a significant increase in a smaller number of reduced DOS features that accumulated during the incubation. Although not significant (t-test p-value > 0.05), there was a small shift in m/z towards smaller DOS features that accumulated relative to those that were lost.

## Discussion

### Preferential loss of reduced $DOS_{SPE}$ in the surface ocean

Organic sulfur can supply the entirety of bacterial sulfur demand in the surface ocean (Kiene and Linn 2000), making it just as biologically active as the other macronutrients in marine DOM. The increase in C:S ratios of $DOM_{SPE}$ with depth reported here, from 243 ± 22 to 289 ± 18, is similar to that of previous observations in the top 200 m, suggesting a preferential remineralization of DOS relative to DOC (Ksionzek et al. 2016). Oxidized OS species account for a majority of $DOM_{SPE}$, but reduced OS species (disulfides and alkyl sulfides) significantly decrease

with depth in the top 200 m. We posit that this demonstrates a preferential remineralization of $DOM_{SPE}$ based not only on heteroatom content (Ksionzek et al. 2016; Phillips et al. 2022), but also on oxidation state of the OS.

Alkyl sulfides and disulfides appear to be rapidly transformed in the surface ocean, decreasing by ~76% and ~77%, respectively, between surface (<10 m) and deep (>150 m) samples. This suggests that these reduced species are produced near the surface at a rate greater than consumption and are subsequently metabolized and/or transformed by microbial consumption at depths below. Sulfonates are the most abundant components of marine $DOS_{SPE}$. While the relative abundance of this oxidized group is lowest in surface samples (<10 m; Fig. 2), the total concentrations are ~20% lower at depth than at the surface (Fig. 3). This suggests that a portion of oxidized OS is also consumed at depth, but, in contrast to the reduced species, a larger reservoir of sulfonates accumulates to become a dominant component of marine $DOM_{SPE}$.

Reduced OS compounds that are lost with depth could include biologically active S metabolites, such as the amino acids cysteine and methionine, as well as others such as glutathione, DMSP, gonyol, thiamine, and biotin (Moran and Durham 2019). These are released to the ocean DOM pool via passive or active exudation of metabolites across cell membranes (Flynn et al. 2008; Moran and Durham 2019) and/or as a result of zooplankton grazing and viral lysis (Dacey and Wakeham 1986; Moran and Durham 2019) and can be rapidly assimilated by marine bacteria (Kiene and Linn 2000; Valle et al. 2015; Moran and Durham 2019). Oxidized OS metabolites, such as taurine, cysteate, DHPS, or isethionate, are just as common as reduced OS metabolites and are often assimilated as carbon sources (Clifford et al. 2017; Moran and Durham 2019), and they may be in part responsible for the concurrent but smaller decrease in oxidized OS with depth. At the same time, DOM reworking might be anticipated to lead to the net oxygenation of OS, for

example from thiols to sulfoxides and sulfonates, replenishing the sulfonate pool from a different source. Sulfonates are well-documented oxidation products of reduced OS compounds, which can occur both biotically (e.g., production of C3 sulfonates (Durham et al. 2019)) and abiotically, (e.g. oxidation of cysteine to sulfonic acid/sulfonate (Phillips et al. 2021)). Ultimately, we find that there is a relatively large pool of compositionally intriguing sulfonates that are SPE-amenable. These compounds are likely the products of re-working, such as from the oxidation of reduced $DOS_{SPE}$ compounds or from aggregation. In contrast, a much smaller reservoir of reduced OS species persists in deeper waters, which could include both biogenic materials and the products of sulfurization reactions in anoxic sediments (Pohlabeln et al. 2017).

**Enigmatic OS groups may be components of long-lived DOM**

Aromatic OS, which previous studies have suggested may be a component of DOS (Pohlabeln and Dittmar 2015), is the second most abundant species in marine $DOM_{SPE}$ after sulfonates but exhibits a much larger ~48% decrease in concentration between surface samples and deep (>150 m) samples. This suggests that aromatic S compounds are primarily sourced from the surface ocean and are lost with depth. Sources of aromatic OS in the biosphere and ocean remain poorly understood. Aromatic OS is a common constituent of relatively mature kerogen in rocks (Raven et al. 2023). In the modern marine water column, sources of aromatic OS likely include cyclization products of sulfurized compounds (Pohlabeln et al. 2017), photochemical production of aromatic S from sulfurized compounds (Stubbins et al. 2010; Pohlabeln et al. 2017), and the microbial re-working of sinking marine particles (Raven et al. 2021), while sinks include photochemical degradation (Kujawinski et al. 2004; Stubbins et al. 2010; Gomez-Saez et al. 2017) and microbial uptake (Matos Neto et al. 2023). Larger dissolved aromatic compounds may also be lost to precipitation and/or flocculation because of interactions with particulate organic matter

(POM) (Kramer et al. 2012). Their high abundance in environmental $DOS_{SPE}$ samples likely reflects selective accumulation of certain aromatic components due to their recalcitrance.

The concentrations of sulfate esters in $DOM_{SPE}$ are small but show a unique pattern relative to the other OS species. Sulfate ester concentrations are significantly higher at the 30 – 80 m depth than at the surface, but their concentrations are consistent between the 30 – 80 m and deeper (150 – 205 m) samples. This suggests that sulfate esters may have relatively long residence times in the surface ocean. Earlier studies have similarly found that some sulfate esters, such as fucoidan, are resistant to microbial breakdown in marine environments (Buck-Wiese et al. 2023). Notably, unlike sulfoxides and sulfonates, sulfate esters have a R–O–S bond and thus cannot be directly produced by the oxidation of reduced OS species like thiols. Therefore, they are likely to represent primary biogenic components of OS, which could include abundant sulfated polysaccharides (fucoidan, carrageenan, and glucuronomannan) or other metabolites, such as choline-*O*-sulfate, an osmolyte produced by a small number of marine microorganisms (Durham et al. 2019; Moran and Durham 2019). While many small, oxidized metabolites are rapidly cycled in the surface ocean, some oxidized components appear to have increased resistance to microbial breakdown, which may contribute to the observed longevity of a portion of marine DOM.

**Local sedimentary sources drive $DOS_{SPE}$ isotopic variability**

We observe a >5‰ range in the $\delta^{34}S$ values of $DOM_{SPE}$ across our study region. A primary driver of this variability is location either on- or off the shelf, which may reflect an influx of sulfurized porewater DOM from the sediments that is most visible in on-shelf samples collected near the seafloor. Generally, sulfurized porewater DOM is expected to be $^{34}S$-depleted compared to biogenic DOM due to the incorporation of $^{34}S$-depleted sulfide released by microbial sulfate reduction. Only a small number of coastal estuarine sediment porewater DOM samples have been

previously measured for $\delta^{34}S$, with values ranging from -2.7 to +0.7‰ (Phillips et al. 2022). Porewater DOM is often sulfur rich, with C:S molar ratios ranging between 40 and 45 (Phillips et al. 2022). Water column samples from previously studied estuaries have C:S and $\delta^{34}S$ values that are indicative of mixing of sediment sulfurized DOM with background seawater DOM (Phillips et al. 2022). Sulfur isotope measurements of marine carbonyl sulfide and carbon disulfide — both produced from marine DOS — also indicate that sulfurized DOS from sediment porewater influences the $\delta^{34}S$ values of samples collected near estuaries or coastal sediments (Davidson et al. 2025). Therefore, the relatively $^{34}S$-depleted DOM compositions that we observe over the shelf are consistent with an increased contribution of sulfurized porewater DOM in on-shelf stations compared to off-shelf stations. $DOM_{SPE}$ from on-shelf stations was both more $^{34}S$-depleted ($\delta^{34}S$ = 14.9 ± 1.3‰) and more sulfur-rich (C:S = 226 ± 20) compared to off-shelf stations ($\delta^{34}S$ = 16.3 ± 1.1‰, C:S = 263 ± 30). Notably, the most $^{34}S$-depleted sample (C1N1) is the sample taken closest (5 m proximity) to the sediment-water interface.

Water mass variation may also play a role in observed on- versus off-shelf differences. On- and off-shelf stations are in distinct water masses (Fig. S5), which may receive DOS inputs with varying $\delta^{34}S$ values due to differing fluxes of terrestrial and sulfurized porewater DOM. Variability in local nutrient availability between water masses could influence the dominant local primary producers at each station. As shown in Fig. 4, $\delta^{34}S$ values of exudates differ among monocultures, suggesting that environmental community composition could be a direct source of S isotopic variability.

$DOS_{SPE}$ speciation is consistent with greater inputs of sulfurized DOM at the on-shelf stations. Specifically, the average calculated concentrations and relative abundances of alkyl sulfides and disulfides, which are thought to be common sulfurization products (Eglinton et al.

1994; Raven et al. 2021), are higher (t-test, $p < 0.001$) at on-shelf stations (75 ± 25 nM S) than off-shelf stations (29 ± 14 nM S), which demonstrates that we may be able to identify localized inputs of sulfurized DOM at on-shelf stations. In addition, the concentration of aromatic S compounds, which may be sulfurization products, are higher on the shelf (Pohlabeln et al. 2017). However, we do not observe a significant correlation between $\delta^{34}S$ values and the relative abundance of disulfides, indicating that the total contribution of sulfurized DOM molecules remains small and/or that these molecules are rapidly oxidized in the oxic ocean. Ultimately, this suggests that although sulfurized DOM products are a minor contributor in the global DOM budget and may be rapidly oxidized, some sediment-derived sulfurized products may persist locally, especially near the sediment-water interface or in anoxic shelf settings.

**$DOM_{SPE}$ $\delta^{34}S$ is less variable than OS oxidation state**

Our samples were collected approximately >1000 km northwest of a previously sampled profile in the North Atlantic Gyre near Bermuda, where $\delta^{34}S$ values from the top 200 m (n = 3) range from 17.7‰ – 18.9‰ (Phillips et al. 2022). The 12.2‰ – 17.3‰ range of our samples (n = 21) observed here is $^{34}S$-depleted relative to existing surface ocean values.

Despite clear correlations in DOS oxidation states with DOC concentration, we do not observe any systematic change in S isotopic composition of $DOS_{SPE}$ with concentration of oxidized or reduced OS (Fig. S5). Changes in speciation correlating with changes in S isotope composition would be expected if certain oxidation states had diagnostic $\delta^{34}S$ values. For example, sulfurized DOM from sediment porewater contains $^{34}S$-depleted alkyl sulfides and disulfides, and thus inputs of these reduced S compounds drive lower $\delta^{34}S$ values of porewater DOM.

We attribute the decoupling of S speciation and $\delta^{34}S$ values to the fact that the bulk sampling and isotopic measurements produce averaged $\delta^{34}S$ values. This masks inter-compound

or intra-group isotopic variability and can lead to consistent $\delta^{34}S$ values. For example, compounds comprising the oxidized OS pool are produced via different biosynthetic pathways in phototrophs. Sulfate esters are produced from sulfate in the cytoplasm via the 3'-phosphoadenosine 5'-phosphosulfate (PAPS) pathway (Klaassen and Boles 1997), while other oxidized OS compounds, such as sulfonates, can either be synthesized through the reduction of sulfate to sulfite in the chloroplast or via PAPS (Benning 1998). This indicates that at least two source pools with potentially distinct sulfate $\delta^{34}S$ values exist for the biosynthesis of OS compounds; however, such differences cannot be resolved with the techniques employed here.

Observed $\delta^{34}S$ values are also likely a result of rapid cycling and transformations of DOS in the marine environment. Abiotic and biotic processes, including oxidation, heterotrophic uptake, and photochemical reactions, contribute to loss of $DOS_{SPE}$ in the upper 200 m of the water column and shift its bulk chemical speciation. Reworking and transformations of DOS between and within reduced and oxidized S pools can move any initially expressed S isotope signatures to the product. For example, if an alkyl sulfide is oxidized to a sulfonate without a fractionation effect, the $\delta^{34}S$ values of different oxidation state pools may become indistinguishable over time.

The shift in $DOS_{SPE}$ speciation that we observe in the upper 200 m of the water column indicates active uptake and oxidation of labile S metabolites, but these processes do not cause a detectable shift in the S isotope composition of $DOM_{SPE}$. Thus the apparent shifts in the $\delta^{34}S$ value of $DOM_{SPE}$ deeper in the water column that have been observed previously (Phillips et al. 2022) are likely driven by processes operating on ~100 – 1,000+ year timescales, such as longer-term alteration and/or mixing of isotopically distinct DOM sources, that are mechanistically distinct as more recalcitrant DOM is transformed.

**Distinct sulfur speciation in monoculture and marine $DOS_{SPE}$**

505 The $DOS_{SPE}$ exuded by lab-grown monocultures of marine microorganisms is clearly
506 distinct from surface ocean marine $DOS_{SPE}$. Generally, marine $DOS_{SPE}$ is oxidized compared to
507 fresh exudates. Marine $DOS_{SPE}$ contains a relatively large proportion of aromatic S compounds
508 and sulfonates, while exudates generally contain higher relative abundances of reduced OS,
509 especially alkyl sulfides, which include thiols. Notably, however, diatom-derived $DOS_{SPE}$ contains
510 a large portion of sulfonates. One likely source of sulfonates from *Thalassiosira pseudonana* is
511 DHPS, which these organisms synthesize at high concentrations that are an order of magnitude
512 greater than other sulfonates quantified in *Thalassiosira* (Durham et al. 2019). Small amounts of
513 aromatic S are also present in biogenic $DOS_{SPE}$ (Fig. 4), although there are no known biosynthetic
514 pathways that directly produce aromatic OS compounds in these organisms. However,
515 aromatization is also a common part of organic matter aging and net hydrogen loss in sediments
516 (Sinninghe Damste and De Leeuw 1990). Therefore, the abundant aromatic S observed in the
517 environmental $DOS_{SPE}$ samples is instead likely derived from a combination of internal
518 recombination reactions, sulfurization products, photochemical degradation products, the
519 reworking of marine particulate organic matter, or from an as-yet undefined biochemical pathway
520 (Pohlabeln et al. 2017; Raven et al. 2021). Their high abundance in environmental $DOS_{SPE}$ samples
521 likely reflects selective accumulation, potentially due to recalcitrance. In contrast to marine
522 $DOS_{SPE}$, sulfoxides are more abundant in biogenic $DOS_{SPE}$ which may be attributed to OS
523 metabolites, such as dimethyl sulfoxide (DMSO) or dimethylsulfoniopropionate (DMSOP), but
524 the concentrations of these metabolites are typically quite low (Andreae 1980; Thume et al. 2018).
525 The sulfoxides observed in the exudates could also result from oxidation of reduced OS (Phillips
526 et al. 2021). The composition of marine $DOS_{SPE}$ is likely initiated by the biogenic signatures
527 observed in the monoculture $DOS_{SPE}$.

We tested the influence of the short-term ecological reworking of freshly produced OS by growing monocultures of heterotrophic bacteria on DOM harvested from phototroph lysates. In these incubations, heterotrophs are limited to the single species' metabolic capacity and are capable of rapid growth, with doubling times as fast as ~0.7 hours (Fig. S3). Based on our observations of the marine $DOS_{SPE}$, we hypothesized that we would observe a loss of both reduced and oxidized OS molecules, but that some oxidized molecules would accumulate over the course of the incubation. This accumulation of oxidized OS would represent the transformation of freshly produced, reduced DOS into oxidized OS as a result of microbial re-working.

In all incubations, both reduced and oxidized DOS molecules measured using UHPLC-ESI-MSMS were significantly depleted from the growth media, indicating that the DOS substrates were taken up by the heterotrophs for metabolism. This depletion is consistent with our observation of the loss of both reduced and oxidized $DOS_{SPE}$ in the surface ocean, where microbial remineralization drives the loss of labile DOS. A small number of reduced DOS features emerged at the end of the incubations, indicating that heterotrophs can also be a source of OS. This aligns with our observations of heterotroph-derived $DOS_{SPE}$ in monoculture, where heterotrophs primarily exude disulfide and alkyl sulfide compounds, along with sulfoxides, some of which are likely oxidation products of reduced OS. In contrast, albeit a limited number of which were putatively identifiable, all oxidized DOS features were depleted from the growth media (Fig. 4B). Thus, we did not observe any rapid transformations of reduced to oxidized OS and conclude that the net oxidation mechanism in the ocean may require more complex DOM and/or longer time scales to emerge. In the marine environment, OS is transformed into the resulting marine $DOS_{SPE}$ pool by both biotic and abiotic processes – including uptake by the microbial loop, priming, photochemical oxidation, and biotic or abiotic oxidation of reduced OS compounds to sulfonates

and sulfates. This wide range of environmental processes occurs simultaneously and over extended timescales. Like the broader DOM pool (Dittmar et al. 2021), the recalcitrance observed in the DOS pool emerges from a complex suite of biotic and abiotic processes that convert labile DOS to recalcitrant DOS (Tang and Liu 2023). An exception to this observation seems to be sulfate esters, some of which appear to be inherently recalcitrant and resistant to microbial degradation within the timescales captured by this study.

### $^{34}$S–enrichment of monoculture DOS$_{SPE}$

We observe that marine DOS$_{SPE}$ is $^{34}$S-depleted by 3.7 – 8.8‰ relative to seawater sulfate (~21‰) (Fig. 1G). Given the role of primary producers in generating DOS, we hypothesized that biogenic DOS would have an isotope composition matching marine DOS$_{SPE}$ (Phillips et al. 2022). This isotopic signal has been observed in biomass (POS), which typically has $\delta^{34}$S values that are slightly $^{34}$S-depleted relative to sulfate (Kaplan et al. 1963; Kaplan and Rittenberg 1964; Phillips et al. 2021). Nevertheless, we note that solid biomass and DOM$_{SPE}$ from monoculture are not directly comparable because SPE recovers only a selective fraction of the dissolved pool (Johnson et al. 2017). Measurements of monoculture biomass are consistent with these earlier observations; they are $^{34}$S-depleted by 2.1 – 5.7‰ relative to sulfate (Fig. 4A). Surprisingly, we find that monoculture exudate DOS$_{SPE}$ is $^{34}$S-enriched relative to sulfate by as much as 8.6‰ (Fig. 4A). Media PPL blanks did not contain measurable S. The consistent $^{34}$S-enrichment of DOS$_{SPE}$ observed across all four monoculture experiments therefore indicates that at least some constituent of exudate DOS$_{SPE}$ is strongly $^{34}$S-enriched. Exudate DOS$_{SPE}$ accounts for only a small fraction (0.4 – 18%) of the total biogenic OS produced by the monoculture such that, on net, biogenic production remains $^{34}$S-depleted relative to seawater sulfate (see Supplemental Text S3).

573 The formation of $^{34}$S-enriched OS species has been reported previously, where intracellular
574 DMSP is $^{34}$S-enriched relative to sulfate by up to ~3‰ in select taxa of symbiotic protists
575 (Gutierrez-Rodriguez et al. 2017). Here, we hypothesize that exudate $^{34}$S-enrichment arises from
576 kinetic isotope effects (KIEs) associated with a branchpoint in OS biosynthesis (Hayes 2001).
577 Sulfur is incorporated into OS compounds via two major biosynthetic pathways: (1) a non-
578 reductive PAPS pathway, where PAPS transfers its sulfate group to OS, and (2) a reductive
579 pathway in which adenosine phosphosulfate is reduced to sulfite and then to cysteine, from which
580 downstream metabolites are synthesized (Giordano and Raven 2014). Both pathways result in the
581 synthesis of key primary OS metabolites. The non-reductive PAPS pathway produces relatively
582 oxidized compounds such as DHPS, taurine, sulfate esters and SQDG (Klaassen and Boles 1997;
583 Burkart et al. 2000; Tevatia et al. 2015), while the reductive cysteine pathway yields most of the
584 reduced molecules in the cell, including cysteine, methionine, DMSP, and glutathione, (Giordano
585 and Raven 2014). Because of the greater number of transformations involving the sulfur atom, we
586 hypothesize that the observed monoculture $DOS_{SPE}$ $^{34}$S-enrichments reflect KIEs expressed in the
587 reductive, rather than oxidative, pathway (Giordano and Raven 2014).

588 Although some cysteine is incorporated directly into proteins, it is also used to produce
589 downstream metabolites. Both protein incorporation and metabolite biosynthesis produce
590 compounds that are $^{34}$S-depleted by 2–5‰ relative to source sulfate (Osorio-Rodriguez et al. 2021;
591 Phillips et al. 2021). This could produce a relatively $^{34}$S-enriched residual intracellular pool of free
592 cysteine. This $^{34}$S-enriched pool of free cysteine, or similar small thiols, could be responsible for
593 the resulting enrichment of $^{34}$S-enriched exudates observed here. Thiols are abundant and represent
594 key components of DOM in the surface ocean (Fourrier and Dulaquais 2024). Their concentration
595 maxima are typically in the top ~100 m of the water column and have been associated with

chlorophyll-a maxima, supporting a biogenic source (Dupont et al. 2006; Gao and Guéguen 2018). Consistent with this, the alkyl sulfide pool – which, in our study, is operationally defined using standards that include both organic sulfides and thiols – has a higher relative abundance in the monoculture samples than in the marine samples.

However, this putative $^{34}$S-enriched pool is missing from our marine samples. This could occur for several reasons and underscores that the relationship between monoculture exudates and marine DOM is inherently complex. First, many small compounds produced in monocultures are likely relatively labile and would be quickly consumed in the surface ocean and thus difficult to capture in marine samples. Small thiols are particularly bioavailable and are likely rapidly consumed by heterotrophs. Consistent with this idea, reduced OS features are lost over time in our heterotrophic transformation incubation experiments. Given that these small, $^{34}$S-enriched compounds are rapidly consumed in the surface ocean, they are unlikely to leave an isotopic signal in marine $DOM_{SPE}$. Secondly, compounds such as small thiols may be poorly retained in environmental SPE samples due to the greater complexity of the marine sample matrix. In marine samples, competition from the broader array of DOM compounds, many of which may have a high affinity for the PPL resin, could reduce the retention of small thiols. In contrast, the reduced chemical diversity of monoculture DOM may enable more efficient retention of thiols on SPE. Furthermore, marine samples contain a larger proportion of older, re-worked $DOM_{SPE}$; thus, the influence of a small $^{34}$S-enriched pool may be masked by the contribution of complex $DOM_{SPE}$ compounds. For these reasons, the direct comparison of monoculture exudates and marine DOM is challenging; however, studies of monoculture DOM can still provide valuable insights. In particular, monoculture DOM studies can be used in conjunction with characterization of marine DOM to constrain "initial" biogenic DOM and to make inferences about the transformations and

re-working that convert primary exudates into DOM observed in the environment. This study highlights small thiols as an important component of DOM with potentially distinct behavior and isotopic composition, making their direct isotopic measurement a compelling next step for research. Ultimately, this work underscores the value of methods that can resolve the diverse oxidation states of organic S for tracing organic sulfur in the marine environment and presents a framework that can be extended to the study of sulfur cycling in other complex chemical, ecological, and biogeochemical systems.

## Author Contribution Statement

MAC, ELM, AAP, and MRR designed the study. ELM, EBK, and KL collected the samples. ELM, EBK, and MRR secured research funding. All authors contributed to data collection and analysis. MAC and AAP created the figures. MAC wrote the paper with input from all authors.

## Acknowledgments

We thank the chief scientist, Dr. Magdalena Andres, the science party, and the crew of the R/V *Armstrong* (AR62). We are grateful to M. Mathuri and A. Sessions for their assistance with EA-IRMS measurements, to Melissa Kido Soule for assistance with MS analysis, to members of the Raven NOISE Lab at UC Santa Barbara for helpful conversations, and to the staff and scientists at the Stanford Synchrotron Radiation Lightsource. Use of the Stanford Synchrotron Radiation Lightsource, SLAC National Accelerator Laboratory (proposal S-XV-ST-6226) is supported by the U.S. Department of Energy Office of Science, Office of Basic Energy Sciences under Contract No. DE-AC02-76SF00515. The SSRL Structural Molecular Biology Program is supported by the DOE Office of Biological and Environmental Research, and by the National Institutes of Health,

National Institute of General Medical Sciences (P30GM133894). The contents of this publication are solely the responsibility of the authors and do not necessarily represent the official views of NIGMS or NIH. This work was supported by the National Science Foundation (OCE #2143817 to MRR). MAC acknowledges the support from the National Science Foundation Graduate Research Fellowship Program (grant number 2139319). ELM was supported by a Simons Foundation Postdoctoral Fellowship in Marine Microbial Ecology. The Woods Hole Oceanographic Institution provided funding for research cruise AR62.

## Open Research

The data that support the findings of this study are available in the Supporting Information of this article (Datasets S1 and S2). This project is registered at BCO-DMO (project # 920983; https://www.bco-dmo.org/project/920983) and all data are being made available according to the OCE Sample and Data Policy.

## Conflict of Interest Disclosure

Co-author Krista Longnecker is Editor-in-Chief for *Limnology and Oceanography: Methods*, which is not a conflict of interest with the editors of *Limnology and Oceanography* but is disclosed here to be fully transparent. The other authors declare there are no conflicts of interest for this manuscript.

## References

Abdulla, H. A., D. J. Burdige, and T. Komada. 2020. Abiotic formation of dissolved organic sulfur in anoxic sediments of Santa Barbara Basin. Organic Geochemistry **139**: 103879. doi:10.1016/j.orggeochem.2019.05.009

Andreae, M. O. 1980. Dimethylsulfoxide in marine and freshwaters. Limnology and Oceanography **25**: 1054–1063. doi:10.4319/lo.1980.25.6.1054

664 Benning, C. 1998. BIOSYNTHESIS AND FUNCTION OF THE SULFOLIPID
665 SULFOQUINOVOSYL DIACYLGLYCEROL. Annu Rev Plant Physiol Plant Mol Biol
666 **49**: 53–75. doi:10.1146/annurev.arplant.49.1.53
667 Brandsma, J., E. C. Hopmans, C. J. M. Philippart, M. J. W. Veldhuis, S. Schouten, and J. S.
668 Sinninghe Damsté. 2012. Low temporal variation in the intact polar lipid composition of
669 North Sea coastal marine water reveals limited chemotaxonomic value. Biogeosciences
670 **9**: 1073–1084. doi:10.5194/bg-9-1073-2012
671 Broek, T. A. B., B. D. Walker, T. P. Guilderson, and M. D. McCarthy. 2017. Coupled
672 ultrafiltration and solid phase extraction approach for the targeted study of semi-labile
673 high molecular weight and refractory low molecular weight dissolved organic matter.
674 Marine Chemistry **194**: 146–157. doi:10.1016/j.marchem.2017.06.007
675 Buck-Wiese, H. and others. 2023. Fucoid brown algae inject fucoidan carbon into the ocean.
676 Proceedings of the National Academy of Sciences **120**: e2210561119.
677 doi:10.1073/pnas.2210561119
678 Burkart, M. D., M. Izumi, E. Chapman, C.-H. Lin, and C.-H. Wong. 2000. Regeneration of
679 PAPS for the Enzymatic Synthesis of Sulfated Oligosaccharides. J. Org. Chem. **65**:
680 5565–5574. doi:10.1021/jo000266o
681 Clifford, E. L., D. A. Hansell, M. M. Varela, M. Nieto-Cid, G. J. Herndl, and E. Sintes. 2017.
682 Crustacean zooplankton release copious amounts of dissolved organic matter as taurine in
683 the ocean. Limnology and Oceanography **62**: 2745–2758. doi:10.1002/lno.10603
684 Cutter, G. A., L. S. Cutter, and K. C. Filippino. 2004. Sources and cycling of carbonyl sulfide in
685 the Sargasso Sea. Limnology and Oceanography **49**: 555–565.
686 doi:10.4319/lo.2004.49.2.0555

687 Dacey, J. W. H., and S. G. Wakeham. 1986. Oceanic Dimethylsulfide: Production During
688 Zooplankton Grazing on Phytoplankton. Science **233**: 1314–1316.
689 doi:10.1126/science.233.4770.1314
690 Davidson, C., A. Angert, Y. Avidani, S. T. Lennartz, M. von Hobe, and A. Amrani. 2025.
691 Sources of marine carbonyl sulfide and its precursors traced by sulfur isotopes.
692 Limnology and Oceanography **n/a**. doi:10.1002/lno.70196
693 Dittmar, T., B. Koch, N. Hertkorn, and G. Kattner. 2008. A simple and efficient method for the
694 solid-phase extraction of dissolved organic matter (SPE-DOM) from seawater.
695 Limnology and Oceanography: Methods **6**: 230–235. doi:10.4319/lom.2008.6.230
696 Dittmar, T., S. T. Lennartz, H. Buck-Wiese, D. A. Hansell, C. Santinelli, C. Vanni, B. Blasius,
697 and J.-H. Hehemann. 2021. Enigmatic persistence of dissolved organic matter in the
698 ocean. Nat Rev Earth Environ **2**: 570–583. doi:10.1038/s43017-021-00183-7
699 Dupont, C. L., James. W. Moffett, R. R. Bidigare, and B. A. Ahner. 2006. Distributions of
700 dissolved and particulate biogenic thiols in the subartic Pacific Ocean. Deep Sea
701 Research Part I: Oceanographic Research Papers **53**: 1961–1974.
702 doi:10.1016/j.dsr.2006.09.003
703 Durham, B. P. and others. 2019. Sulfonate-based networks between eukaryotic phytoplankton
704 and heterotrophic bacteria in the surface ocean. Nat Microbiol **4**: 1706–1715.
705 doi:10.1038/s41564-019-0507-5
706 Eglinton, T. I., J. E. Irvine, A. Vairavamurthy, W. Zhou, and B. Manowitz. 1994. Formation and
707 diagenesis of macromolecular organic sulfur in Peru margin sediments. Organic
708 Geochemistry **22**: 781–799. doi:10.1016/0146-6380(94)90139-2

709 Flynn, K. J., D. R. Clark, and Y. Xue. 2008. Modeling the Release of Dissolved Organic Matter
710 by Phytoplankton. Journal of Phycology **44**: 1171–1187. doi:10.1111/j.1529-
711 8817.2008.00562.x
712 Fourrier, P., and G. Dulaquais. 2024. Low-molecular-weight reduced sulfur substances: A major
713 component of nonvolatile dissolved organic sulfur in the Pacific Ocean. Limnol
714 Oceanogr Letters **9**: 735–744. doi:10.1002/lol2.10417
715 Galí, M., E. Devred, M. Levasseur, S.-J. Royer, and M. Babin. 2015. A remote sensing algorithm
716 for planktonic dimethylsulfoniopropionate (DMSP) and an analysis of global patterns.
717 Remote Sensing of Environment **171**: 171–184. doi:10.1016/j.rse.2015.10.012
718 Gao, Z., and C. Guéguen. 2018. Distribution of thiol, humic substances and colored dissolved
719 organic matter during the 2015 Canadian Arctic GEOTRACES cruises. Marine
720 Chemistry **203**: 1–9. doi:10.1016/j.marchem.2018.04.001
721 Giordano, M., and J. A. Raven. 2014. Nitrogen and sulfur assimilation in plants and algae.
722 Aquatic Botany **118**: 45–61. doi:10.1016/j.aquabot.2014.06.012
723 Gomez-Saez, G. V., A. M. Pohlabeln, A. Stubbins, C. M. Marsay, and T. Dittmar. 2017.
724 Photochemical Alteration of Dissolved Organic Sulfur from Sulfidic Porewater. Environ.
725 Sci. Technol. **51**: 14144–14154. doi:10.1021/acs.est.7b03713
726 Guillard, R. R. L. 1975. Culture of Phytoplankton for Feeding Marine Invertebrates, p. 29–60. *In*
727 W.L. Smith and M.H. Chanley [eds.], Culture of Marine Invertebrate Animals:
728 Proceedings — 1st Conference on Culture of Marine Invertebrate Animals Greenport.
729 Springer US.

730 Guillard, R. R. L., and J. H. Ryther. 1962. STUDIES OF MARINE PLANKTONIC DIATOMS:
731 I. CYCLOTELLA NANA HUSTEDT, AND DETONULA CONFERVACEA (CLEVE)
732 GRAN. Can. J. Microbiol. **8**: 229–239. doi:10.1139/m62-029
733 Gutierrez-Rodriguez, A., L. Pillet, T. Biard, W. Said-Ahmad, A. Amrani, R. Simó, and F. Not.
734 2017. Dimethylated sulfur compounds in symbiotic protists: A potentially significant
735 source for marine DMS(P). Limnology and Oceanography **62**: 1139–1154.
736 doi:10.1002/lno.10491
737 Halewood, E., K. Opalk, L. Custals, M. Carey, D. A. Hansell, and C. A. Carlson. 2022.
738 Determination of dissolved organic carbon and total dissolved nitrogen in seawater using
739 High Temperature Combustion Analysis. Front. Mar. Sci. **9**.
740 doi:10.3389/fmars.2022.1061646
741 Hansell, D. A. 2013. Recalcitrant Dissolved Organic Carbon Fractions. Annual Review of
742 Marine Science **5**: 421–445. doi:10.1146/annurev-marine-120710-100757
743 Hayes, J. 2001. Fractionation of the Isotopes of the Isotopes of the Isotopes of Carbon and Hy
744 Carbon and Hy Carbon and Hydrogen in Biosynthetic Pr in Biosynthetic Processes.
745 Mineralogical Society of America.
746 Hertkorn, N., M. Harir, B. P. Koch, B. Michalke, and P. Schmitt-Kopplin. 2013. High-field
747 NMR spectroscopy and FTICR mass spectrometry: powerful discovery tools for the
748 molecular level characterization of marine dissolved organic matter. Biogeosciences **10**:
749 1583–1624. doi:10.5194/bg-10-1583-2013
750 Ho, T.-Y., A. Quigg, Z. V. Finkel, A. J. Milligan, K. Wyman, P. G. Falkowski, and F. M. M.
751 Morel. 2003. The Elemental Composition of Some Marine Phytoplankton. Journal of
752 Phycology **39**: 1145–1159. doi:10.1111/j.0022-3646.2003.03-090.x

753 Ibrahim, H., and L. Tremblay. 2023. Origin of dissolved organic sulfur in marine waters and the
754 impact of abiotic sulfurization on its composition and fate. Marine Chemistry **254**:
755 104273. doi:10.1016/j.marchem.2023.104273
756 Johnson, W. M., M. C. Kido Soule, and E. B. Kujawinski. 2017. Extraction efficiency and
757 quantification of dissolved metabolites in targeted marine metabolomics. Limnology and
758 Oceanography: Methods **15**: 417–428. doi:10.1002/lom3.10181
759 Johnston, S. E., K. Finlay, R. G. M. Spencer, D. E. Butman, M. Metz, R. Striegl, and M. J.
760 Bogard. 2022. Zooplankton release complex dissolved organic matter to aquatic
761 environments. Biogeochemistry **157**: 313–325. doi:10.1007/s10533-021-00876-7
762 Kaplan, I. R., K. O. Emery, and S. C. Rittenbebg. 1963. The distribution and isotopic abundance
763 of sulphur in recent marine sediments off southern California. Geochimica et
764 Cosmochimica Acta **27**: 297–331. doi:10.1016/0016-7037(63)90074-7
765 Kaplan, I. R., and S. C. Rittenberg. 1964. Microbiological Fractionation of Sulphur Isotopes.
766 Microbiology **34**: 195–212. doi:10.1099/00221287-34-2-195
767 Kido Soule, M. C., K. Longnecker, W. M. Johnson, and E. B. Kujawinski. 2015. Environmental
768 metabolomics: Analytical strategies. Marine Chemistry **177**: 374–387.
769 doi:10.1016/j.marchem.2015.06.029
770 Kieber, D. J., L. C. Powers, A. Stubbins, and W. L. Miller. 2024. Chapter 11 - Marine
771 photochemistry of organic matter: Processes and impacts, p. 507–585. *In* D.A. Hansell
772 and C.A. Carlson [eds.], Biogeochemistry of Marine Dissolved Organic Matter (Third
773 Edition). Academic Press.

774 Kiene, R. P., and L. J. Linn. 2000. The fate of dissolved dimethylsulfoniopropionate (DMSP) in
775 seawater: tracer studies using 35S-DMSP. Geochimica et Cosmochimica Acta **64**: 2797–
776 2810. doi:10.1016/S0016-7037(00)00399-9
777 Klaassen, C. D., and J. W. Boles. 1997. The importance of 3‘-phosphoadenosine 5‘-
778 phosphosulfate (PAPS) in the regulation of sulfation. The FASEB Journal **11**: 404–418.
779 doi:10.1096/fasebj.11.6.9194521
780 Koch, B. P., K. B. Ksionzek, O. J. Lechtenfeld, S. L. McCallister, P. Schmitt-Kopplin, J. K.
781 Geuer, and W. Geibert. 2017. Response to Comment on “Dissolved organic sulfur in the
782 ocean: Biogeochemistry of a petagram inventory.” Science **356**: 813–813.
783 doi:10.1126/science.aam6328
784 Kramer, M. G., J. Sanderman, O. A. Chadwick, J. Chorover, and P. M. Vitousek. 2012. Long-
785 term carbon storage through retention of dissolved aromatic acids by reactive particles in
786 soil. Global Change Biology **18**: 2594–2605. doi:10.1111/j.1365-2486.2012.02681.x
787 Ksionzek, K. B., O. J. Lechtenfeld, S. L. McCallister, P. Schmitt-Kopplin, J. K. Geuer, W.
788 Geibert, and B. P. Koch. 2016. Dissolved organic sulfur in the ocean: Biogeochemistry of
789 a petagram inventory. Science **354**: 456–459. doi:10.1126/science.aaf7796
790 Kujawinski, E. B., R. Del Vecchio, N. V. Blough, G. C. Klein, and A. G. Marshall. 2004.
791 Probing molecular-level transformations of dissolved organic matter: insights on
792 photochemical degradation and protozoan modification of DOM from electrospray
793 ionization Fourier transform ion cyclotron resonance mass spectrometry. Marine
794 Chemistry **92**: 23–37. doi:10.1016/j.marchem.2004.06.038

795 Lana, A. and others. 2011. An updated climatology of surface dimethlysulfide concentrations
796 and emission fluxes in the global ocean. Global Biogeochemical Cycles **25**.
797 doi:10.1029/2010GB003850
798 Lennartz, S. T. and others. 2019. The influence of dissolved organic matter on the marine
799 production of carbonyl sulfide (OCS) and carbon disulfide ($CS_2$) in the Peruvian
800 upwelling. Ocean Science **15**: 1071–1090. doi:10.5194/os-15-1071-2019
801 Matos Neto, G., E. de L. S. Marques, L. K. S. Oliveira, R. P. Rezende, and J. C. T. Dias. 2023.
802 Searching for bacteria able to metabolize polycyclic aromatic sulfur compounds in 12-
803 years periodically fed bioreactor. Arch Microbiol **205**: 336. doi:10.1007/s00203-023-
804 03674-x
805 Moore, L. R. and others. 2007. Culturing the marine cyanobacterium Prochlorococcus.
806 Limnology and Oceanography: Methods **5**: 353–362. doi:10.4319/lom.2007.5.353
807 Moran, M. A. and others. 2022. The Ocean's labile DOC supply chain. Limnology and
808 Oceanography **67**: 1007–1021. doi:10.1002/lno.12053
809 Moran, M. A., and B. P. Durham. 2019. Sulfur metabolites in the pelagic ocean. Nat Rev
810 Microbiol **17**: 665–678. doi:10.1038/s41579-019-0250-1
811 Osorio-Rodriguez, D., M. Razo-Mejia, N. F. Dalleska, A. L. Sessions, V. J. Orphan, and J. F.
812 Adkins. 2021. Sulfur isotope fractionations constrain the biological cycling of
813 dimethylsulfoniopropionate in the upper ocean. Limnology and Oceanography **66**: 3607–
814 3618. doi:10.1002/lno.11901
815 Ossola, R., J. Tolu, B. Clerc, P. R. Erickson, L. H. E. Winkel, and K. McNeill. 2019.
816 Photochemical Production of Sulfate and Methanesulfonic Acid from Dissolved Organic
817 Sulfur. Environ. Sci. Technol. **53**: 13191–13200. doi:10.1021/acs.est.9b04721

Petras, D. and others. 2017. High-Resolution Liquid Chromatography Tandem Mass Spectrometry Enables Large Scale Molecular Characterization of Dissolved Organic Matter. Front. Mar. Sci. **4**. doi:10.3389/fmars.2017.00405

Phillips, A. A. and others. 2022. Novel sulfur isotope analyses constrain sulfurized porewater fluxes as a minor component of marine dissolved organic matter. Proceedings of the National Academy of Sciences **119**: e2209152119. doi:10.1073/pnas.2209152119

Phillips, A. A., F. Wu, and A. L. Sessions. 2021. Sulfur isotope analysis of cysteine and methionine via preparatory liquid chromatography and elemental analyzer isotope ratio mass spectrometry. Rapid Comm Mass Spectrometry **35**: e9007. doi:10.1002/rcm.9007

Pohlabeln, A. M., and T. Dittmar. 2015. Novel insights into the molecular structure of non-volatile marine dissolved organic sulfur. Marine Chemistry **168**: 86–94. doi:10.1016/j.marchem.2014.10.018

Pohlabeln, A. M., G. V. Gomez-Saez, B. E. Noriega-Ortega, and T. Dittmar. 2017. Experimental Evidence for Abiotic Sulfurization of Marine Dissolved Organic Matter. Front. Mar. Sci. **4**. doi:10.3389/fmars.2017.00364

Raven, M. R. 2025. The Marine Organic Sulfur Cycle.doi:10.1146/annurev-marine-040124-105229

Raven, M. R., P. W. Crockford, M. S. W. Hodgskiss, T. W. Lyons, C. J. Tino, and S. M. Webb. 2023. Organic matter sulfurization and organic carbon burial in the Mesoproterozoic. Geochimica et Cosmochimica Acta **347**: 102–115. doi:10.1016/j.gca.2023.02.020

Raven, M. R., R. G. Keil, and S. M. Webb. 2021. Microbial sulfate reduction and organic sulfur formation in sinking marine particles. Science **371**: 178–181. doi:10.1126/science.abc6035

Riedel, T., M. Zark, A. V. Vähätalo, J. Niggemann, R. G. M. Spencer, P. J. Hernes, and T. Dittmar. 2016. Molecular Signatures of Biogeochemical Transformations in Dissolved Organic Matter from Ten World Rivers. Front. Earth Sci. **4**. doi:10.3389/feart.2016.00085

Sabadel, A. J. M., T. J. Browning, D. Kruimer, R. L. Airs, E. M. S. Woodward, R. Van Hale, and R. D. Frew. 2017. Determination of picomolar dissolved free amino acids along a South Atlantic transect using reversed-phase high-performance liquid chromatography. Marine Chemistry **196**: 173–180. doi:10.1016/j.marchem.2017.09.008

Sinninghe Damste, J. S., and J. W. De Leeuw. 1990. Analysis, structure and geochemical significance of organically-bound sulphur in the geosphere: State of the art and future research. Organic Geochemistry **16**: 1077–1101. doi:10.1016/0146-6380(90)90145-P

Stubbins, A. and others. 2010. Illuminated darkness: Molecular signatures of Congo River dissolved organic matter and its photochemical alteration as revealed by ultrahigh precision mass spectrometry. Limnology and Oceanography **55**: 1467–1477. doi:10.4319/lo.2010.55.4.1467

Tang, K., and L. Liu. 2023. Bacteria are driving the ocean's organosulfur cycle. Trends in Microbiology **31**: 772–775. doi:10.1016/j.tim.2023.05.003

Tevatia, R., J. Allen, D. Rudrappa, D. White, T. E. Clemente, H. Cerutti, Y. Demirel, and P. Blum. 2015. The taurine biosynthetic pathway of microalgae. Algal Research **9**: 21–26. doi:10.1016/j.algal.2015.02.012

Thume, K., B. Gebser, L. Chen, N. Meyer, D. J. Kieber, and G. Pohnert. 2018. The metabolite dimethylsulfoxonium propionate extends the marine organosulfur cycle. Nature **563**: 412–415. doi:10.1038/s41586-018-0675-0

Tripp, H. J., J. B. Kitner, M. S. Schwalbach, J. W. H. Dacey, L. J. Wilhelm, and S. J. Giovannoni. 2008. SAR11 marine bacteria require exogenous reduced sulphur for growth. Nature **452**: 741–744. doi:10.1038/nature06776

Vairavamurthy, A. 1998. Using X-ray absorption to probe sulfur oxidation states in complex molecules. Spectrochimica Acta Part A: Molecular and Biomolecular Spectroscopy **54**: 2009–2017. doi:10.1016/S1386-1425(98)00153-X

Valle, D. A. del, S. Martínez-García, S. A. Sañudo-Wilhelmy, R. P. Kiene, and D. M. Karl. 2015. Methionine and dimethylsulfoniopropionate as sources of sulfur to the microbial community of the North Pacific Subtropical Gyre. Aquatic Microbial Ecology **75**: 103–116. doi:10.3354/ame01750

Vihtakari, M. 2024. ggOceanMaps: Plot Data on Oceanographic Maps using "ggplot2."

Webb, S. M. 2005. SIXpack: a graphical user interface for XAS analysis using IFEFFIT. Phys. Scr. **2005**: 1011. doi:10.1238/Physica.Topical.115a01011

Weber, L., M. Armenteros, M. Kido Soule, K. Longnecker, E. B. Kujawinski, and A. Apprill. 2020. Extracellular Reef Metabolites Across the Protected Jardines de la Reina, Cuba Reef System. Front. Mar. Sci. **7**. doi:10.3389/fmars.2020.582161

Wohl, C. and others. 2024. Marine emissions of methanethiol increase aerosol cooling in the Southern Ocean. Science Advances **10**: eadq2465. doi:10.1126/sciadv.adq2465

Zhang, X.-H., J. Liu, J. Liu, G. Yang, C.-X. Xue, A. R. J. Curson, and J. D. Todd. 2019. Biogenic production of DMSP and its degradation to DMS-their roles in the global sulfur cycle. Sci China Life Sci **62**: 1296–1319. doi:10.1007/s11427-018-9524-y

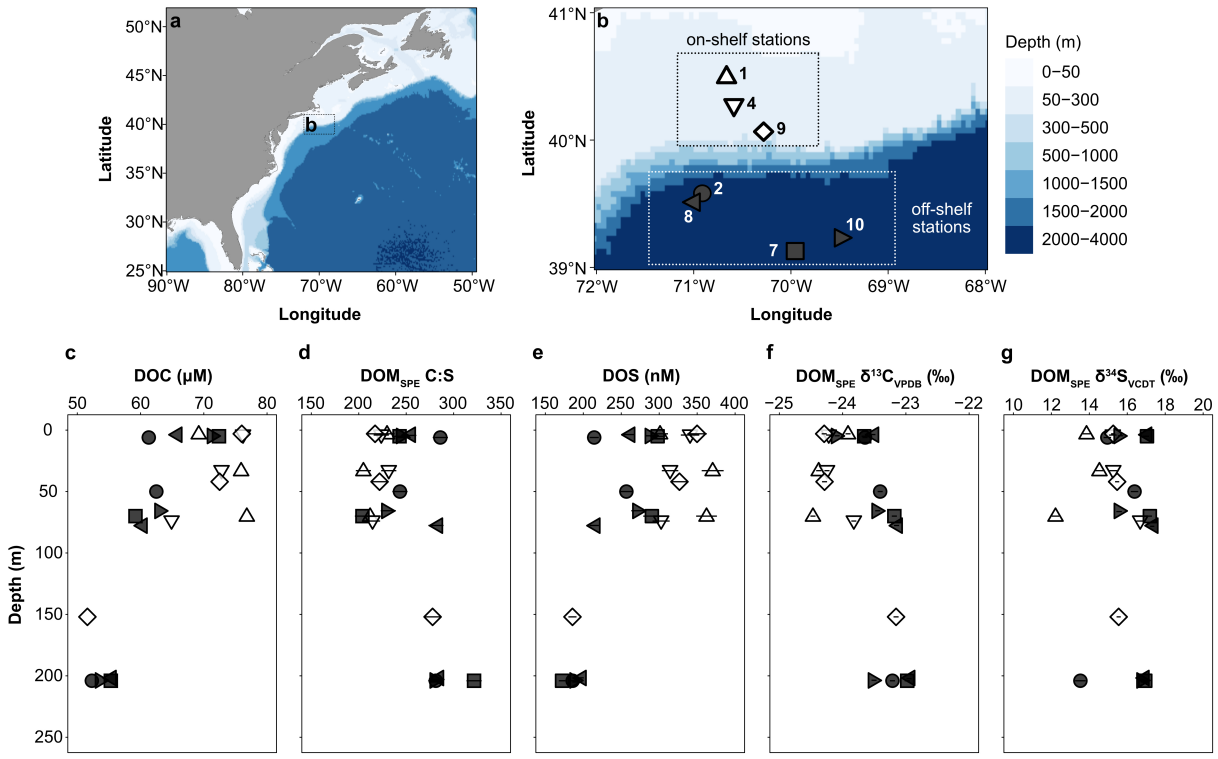


885

886 **Figure 1**. DOS sampling locations and geochemical characteristics. (**a**) Map of sampling region
887 relative to the East coast of the United States. (**b**) Enlarged view of North Atlantic sampling region
888 showing the sampling stations. Maps were generated with ggOceanMaps (Vihtakari 2024).
889 Profiles were collected at three stations on the continental shelf (water depth <200 m; stations 1,
890 4, and 9; white symbols) and four stations off the shelf (water depth >2,000 m, stations 2, 7, 8, and
891 10; black symbols). DOM properties plotted against depth, including: (**c**) concentrations of DOC,
892 (**d**) molar ratios of C:S in $DOM_{SPE}$, (**e**) calculated DOS concentration, (**f**) $\delta^{13}C$ values of $DOM_{SPE}$,

and (**g**) $\delta^{34}S$ values of $DOM_{SPE}$. 1σ errors are shown in (d – g). Symbol shapes correspond with the stations shown in (b).

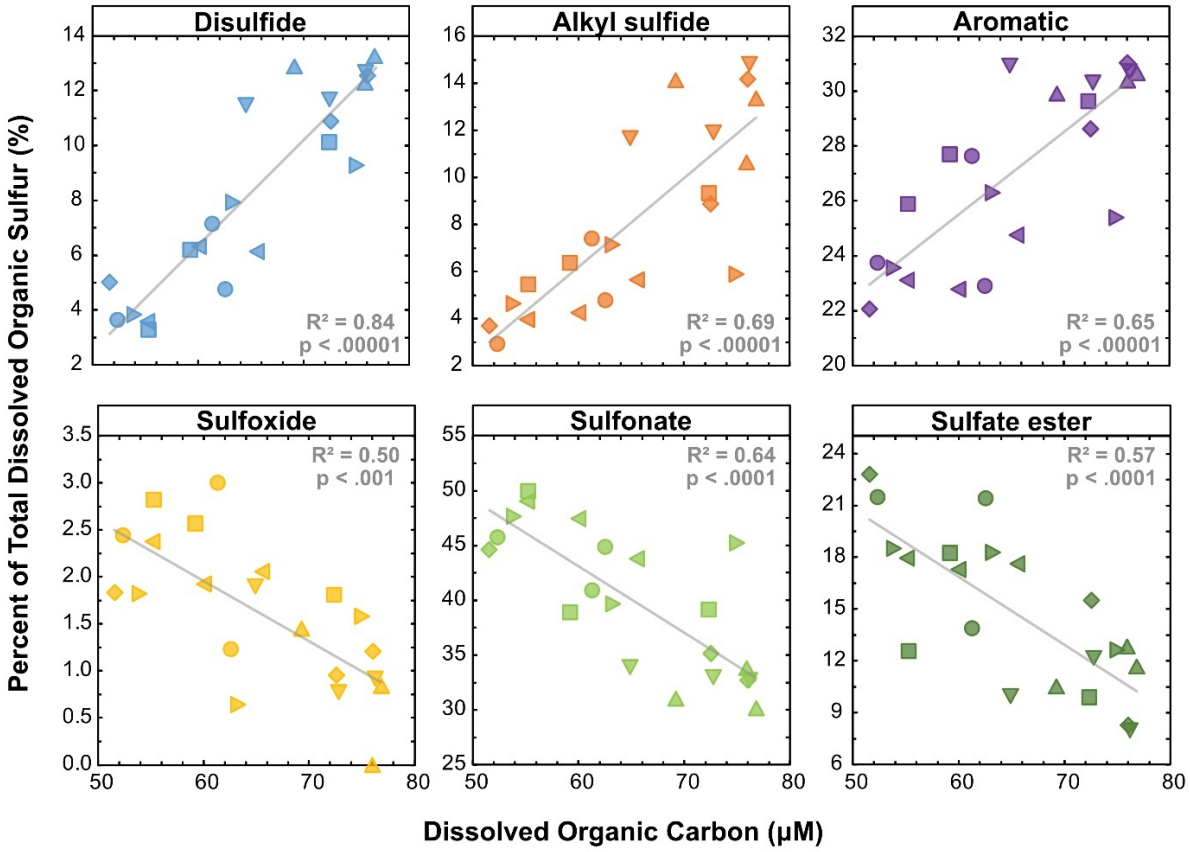


**Figure 2.** Correlations between DOC concentration and $DOS_{SPE}$ OS oxidation state in the North Atlantic. X-axes show concentrations of DOC. Y-axes show the percentage of total DOS present in each oxidation index state. Reduced OS compounds (disulfides, alkyl sulfides, aromatic S) are shown on the top row, and oxidized OS compounds (sulfoxide, sulfonate, sulfate ester) are shown in the bottom row. Note the variable scale on the y-axes. Symbol shapes correspond with stations shown in Fig. 1b. DOC is a proxy for depth (DOC decreases with depth), so positively correlated plots show surface water enrichment, and the negative correlations show deep water enrichment. The Pearson correlation coefficient ($R^2$) and p-value are reported for each OS species. 1σ errors

904 are smaller than the symbol for DOC concentrations; fit uncertainties are ± <2% for S speciation
905 (Vairavamurthy 1998).

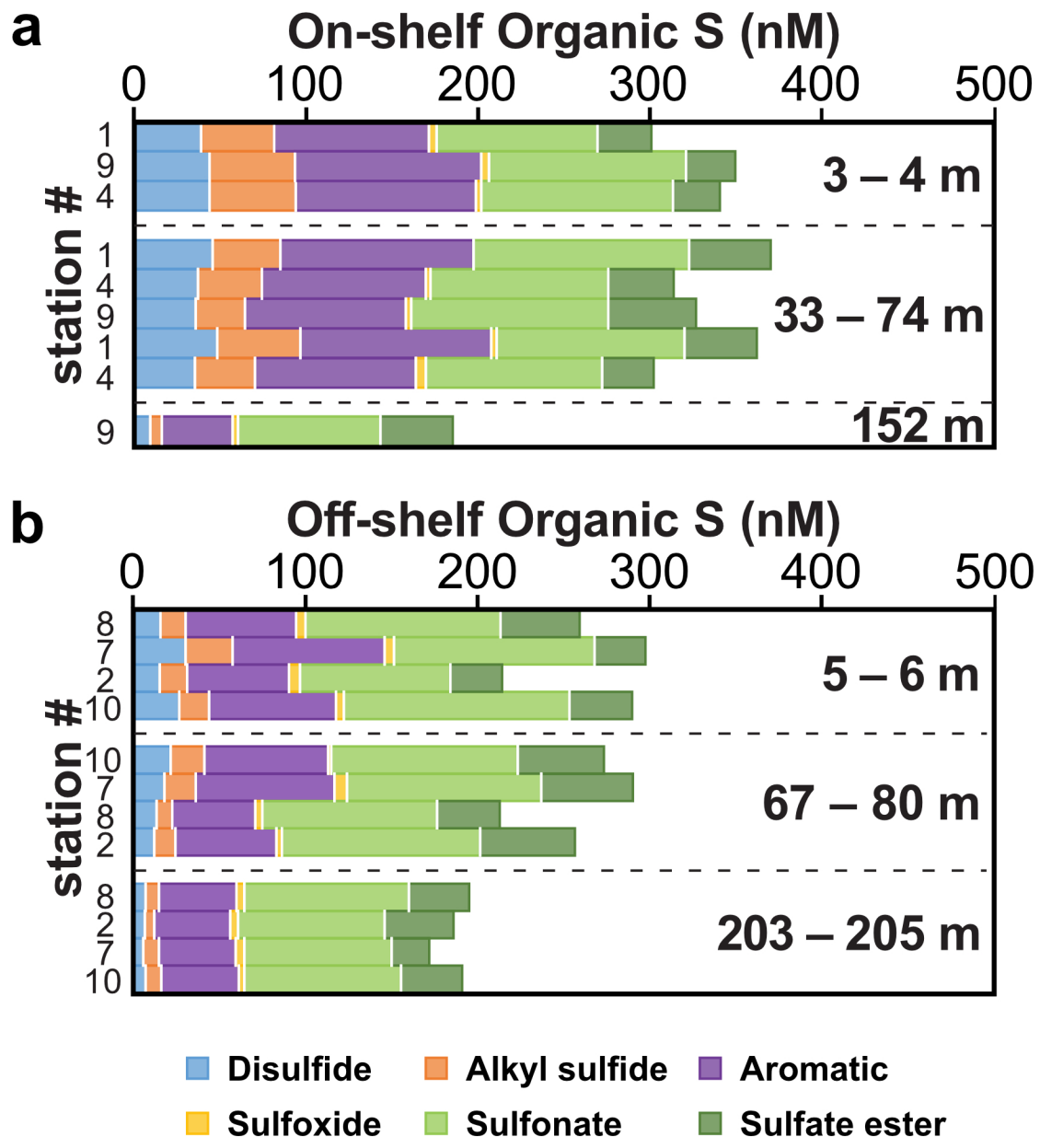


906

907 **Figure 3.** Depth trends in the abundance and oxidation state of $DOS_{SPE}$. From the (**a**) on-shelf
908 stations and (**b**) the off-shelf stations in the North Atlantic. The x-axis shows the concentration of
909 $DOS_{SPE}$ (nM), and the y-axis shows the station number of each sample. The y-axis is arranged in

overall depth order, with depths for each cluster of samples listed at right. Oxidation state distributions are based on fitting to standard spectra (Raven et al., 2021; Vairavamurthy, 1998). Bar charts show the concentrations of $DOS_{SPE}$ in various oxidation states, which were calculated by multiplying the relative abundance of each oxidation state (determined via XAS) by the measured DOC concentration and dividing by the C:S ratio for each sample (Dataset S1).

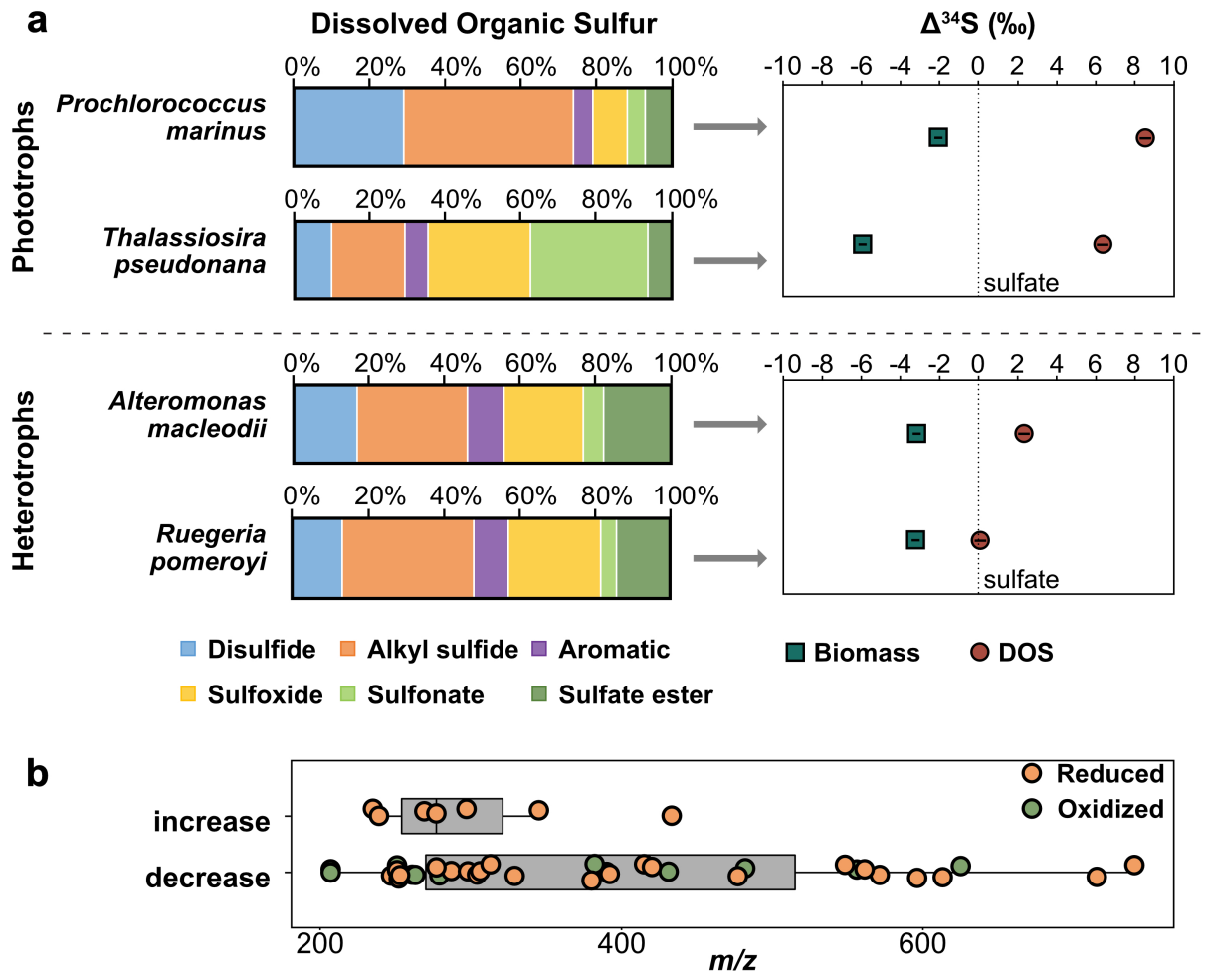


**Figure 4.** OS and isotopic composition of monocultures and results of DOS transformation incubations. (**a**) OS speciation in $DOM_{SPE}$ from triplicate monocultures of representative cyanobacteria, algae, and heterotrophic bacteria. The S isotope composition of monoculture

$DOM_{SPE}$ and particulate biomass with respect to growth media sulfate (source sulfate is normalized to 0‰) is shown to the right of each set of XAS results; analytical uncertainty for $\delta^{34}S$ was 0.2 and 0.1‰, respectively (error bars are smaller than points). (**b**) The mass-to-charge ratio (m/z) of putatively identified OS-containing features that increased (top boxplot) or decreased (bottom boxplot) in at least one of the four DOS incubation experiments. The color of jitter points reflects a putative assignment of S oxidation state of oxidized (green) or reduced (orange) based on fragments and neutral loss of OS-containing fragments in $MS^2$ spectra.